PERGAMON

Solid-State Electronics 45 (2001) 475–482

SOLID-STATE ELECTRONICS

Comparison of titanium and platinum Schottky barrier heights to $Ga_{0.47}In_{0.53}As$ obtained from Franz Keldysh oscillations and Schottky diode characteristics

N. Shamir [a,*], B. Sheinman [a], D. Ritter [a], D. Gershoni [b]

[a] *Department of Electrical Engineering, Technion-Israel Institute of Technology, Technion City, Haifa 32000, Israel*
[b] *The Solid State Institute, Technion-Israel Institute of Technology, Technion City, Haifa 32000, Israel*

Received 19 October 2000; accepted 30 November 2000

Abstract

The Schottky barrier height of Ti and Pt contacts to $Ga_{0.47}In_{0.53}As$ was measured using Franz Keldysh oscillations detected by electro absorption modulation, and compared to values obtained from the Schottky diode current voltage characteristics. Both methods reveal that the Schottky barrier height for holes in Pt contacts is 50–70 meV lower than in Ti contacts. The obtained barrier heights were used to calculate the specific contact resistance of Pt and Ti to p-type $Ga_{0.47}In_{0.53}As$. The results agree well with experimental data. A de-correlation method for improving the resolution of electro absorption data analysis is presented. An experimentally obtained correction factor for the measured electric field is introduced in order to account for a discrepancy between electro absorption theory and experiment. © 2001 Elsevier Science Ltd. All rights reserved.

1. Introduction

In GaInAs based transistors, platinum and titanium are widely used as ohmic contacts to optimize their high frequency performance. The work function of Pt is 1.3 eV higher than that of Ti [1], and accordingly Pt has a lower specific contact resistance to p-type material, and Ti has a lower specific contact resistance to n-type material. However, the difference between the specific contact resistance of the two metals to both n-type and p-type material is much smaller than expected in view of the large difference between their work functions. It is thus evident that the difference in the Schottky barrier height (Fig. 1) between the two metals is much smaller than the difference between their work functions, as found in many other material systems [2]. In this study, the built in potential (Fig. 1) of Ti and Pt GaInAs Schottky diodes was measured using the electro absorption modulation (EAM) technique [3]. A small but well resolved difference of about 50–70 meV between the built in potentials was detected. The measured values of the built in potential were consistent with the current voltage characteristics of the Schottky diodes studied in this work and in previous reports [4]. The specific contact resistance of Ti and Pt to heavily doped p-type GaInAs was measured as well, and found consistent with the measured Schottky barrier height.

2. Crystal growth and device fabrication

The GaInAs layers were grown by a compact metal organic MBE system [5] on 100 oriented InP substrates. The n and p dopant atoms were Sn and Be respectively. The Schottky diode layer structure, described in Fig. 2, consisted of a 140 nm undoped GaInAs layer grown on top of a heavily doped p-type contact layer.

The metals were deposited by electron beam evaporation at pressures lower than 10^{-7} mbar. Before

* Corresponding author. Tel.: +972-4-8655193; fax: +972-4-8323041.
E-mail address: nachums@ee.technion.ac.il (N. Shamir).

0038-1101/01/$ - see front matter © 2001 Elsevier Science Ltd. All rights reserved.
PII: S0038-1101(01)00008-9

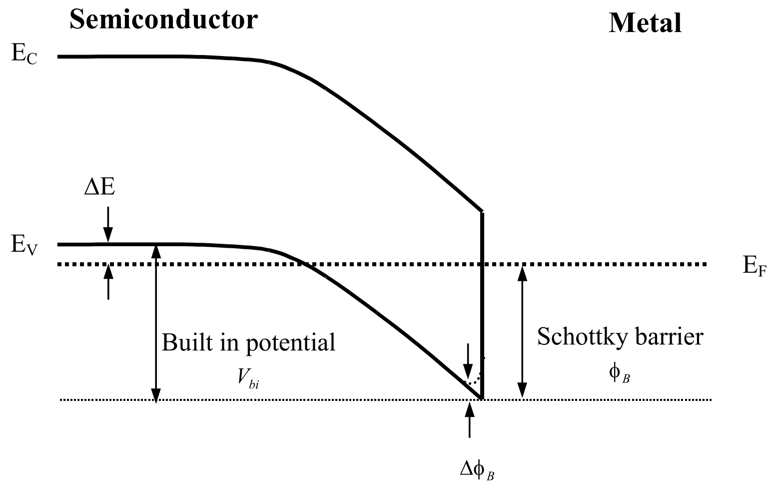

Fig. 1. Energy band diagram of a metal–semiconductor contact.

evaporation, the samples were treated by a 30% HCl solution for two seconds in order to remove the native oxides, rinsed by distilled water for 1 min, and spin-dried. The metal sequences were Ti/Au (100 Å/2000 Å) and Pt/Ti/Pt/Au (50 Å/200 Å/200 Å/2000 Å). In the Pt based contact, the Ti layer is believed to draw the oxides out of the metal semiconductor interface [6]. No contact alloying was carried out.

3. Experimental results

3.1. Electro absorption modulation

The EAM experimental setup is illustrated in Fig. 3. Light from a 100 W quartz tungsten halogen (QTH) lamp was transmitted through a monochromator, collimated by the first lens and focused on the device by

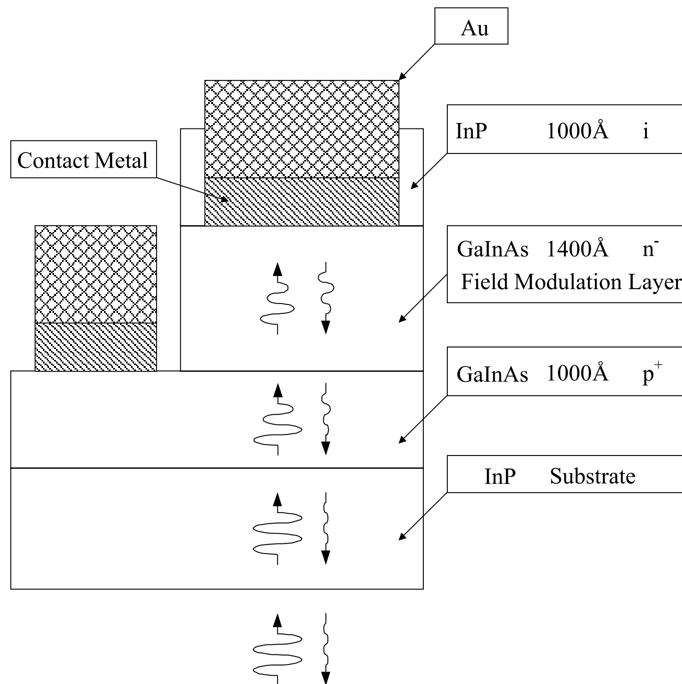

Fig. 2. Schematic description of the Schottky diode structure. In the electro-absorption experiment the light is transmitted through the substrate and reflected by the metal contact.

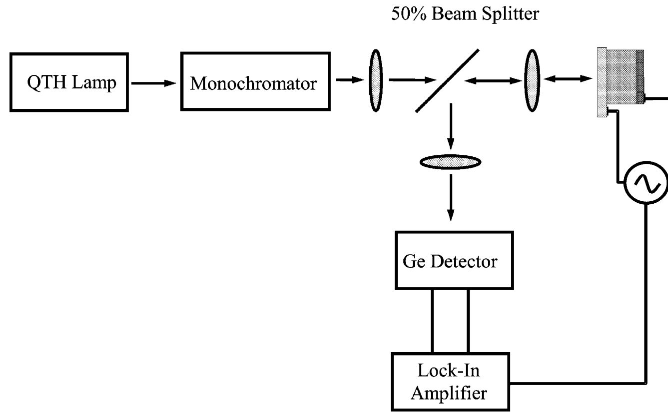

Fig. 3. EAM experimental setup. The incident light was collimated by the first lens and focused on the device by the second lens. A 50% beam splitter diverted the light reflected from the device to a third lens, which focused it on a sensitive Ge detector. Lock-in amplifier, synchronized with the electrical modulation, measured the EAM signal.

the second lens. A 50% beam splitter diverted the light reflected from the device to a third lens, which focused it on a sensitive Ge detector. Photo current measurements were used for precise focal adjustments of the sample mounting. The Schottky diodes were backside illuminated through the InP substrate and the transmitted light was reflected by the metal contacts. This configuration improved the signal to noise ratio because light absorption was doubled compared to a transmission spectroscopy setup. Small signal AC voltage superimposed on DC bias was applied to the device. A lock-in amplifier, synchronized with the electrical modulation, was used for measuring the EAM signal. In this setup we were able to measure light modulation magnitudes of about 5×10^{-5} of the reflected light intensity.

The EAM spectra of the Pt and Ti Schottky diodes were measured for various DC bias levels. The applied bias significantly influenced the observed Franz Keldysh oscillations (FKOs), as demonstrated in Fig. 4. The measured FKOs were independent of the probing light intensity, ruling out photovoltaic effects.

A comparison of the EAM spectra of two diodes at equal bias level is presented in Fig. 5. The clear difference between the FKOs can only be attributed to the difference between the Schottky barrier heights of the Pt and Ti metal–semiconductor contacts. To accurately measure the difference between the built in potentials of the two diodes the DC bias of the Pt diode was varied until the FKO peaks coincided with the FKO peaks of the Ti diode, as demonstrated in Fig. 6. The obtained difference is 50 meV with an error margin of about 20 meV

To evaluate magnitudes of the built in potential and the internal field in the two diodes we use the expression given in [7,8]:

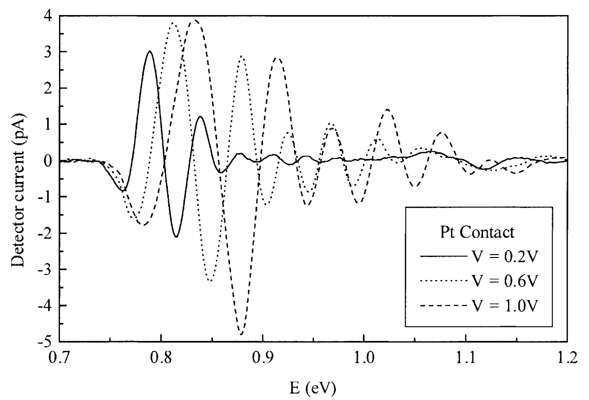

Fig. 4. EAM spectrum measured at different applied DC bias levels. Large spectral shifts are observed with the internal field increase.

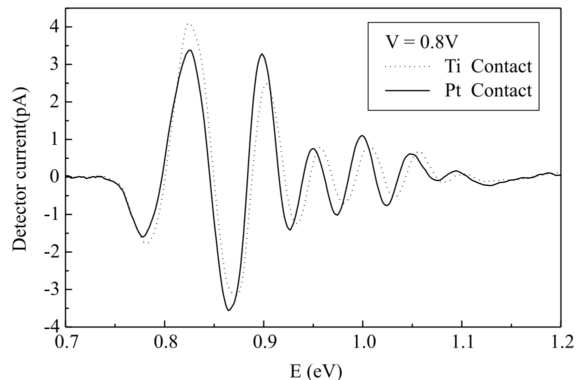

Fig. 5. EAM spectrum of Ti and Pt diodes with an equal reverse bias of 0.8 V. The spectral shift is due to the different contact potential of the two metals.

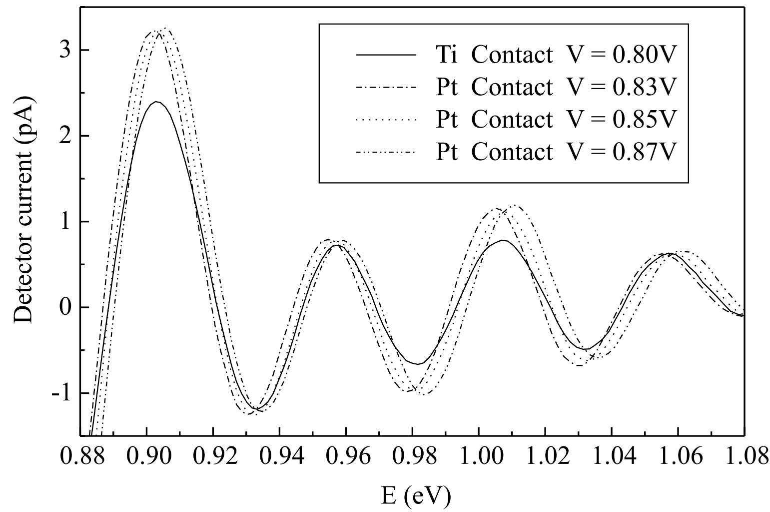

Fig. 6. EAM spectrum of the Ti diode operated at a reverse bias of 0.8 V and the Pt diode operated at varying reverse bias levels. The spectrum of the Pt diode biased at 0.85 V is very similar to that of the Ti diode, indicating that the potential barrier difference is 50 meV.

$$\frac{\Delta R(E)}{R(E)} \propto \exp\left[\frac{-2\Gamma(E-E_g)^{1/2}}{(\hbar\theta)^{3/2}}\right]\cos\left[\frac{4}{3}\frac{(E-E_g)^{3/2}}{(\hbar\theta)^{3/2}}+\chi\right] \times \left[E^2(E-E_g)\right]^{-1} \quad (1)$$

where E is the photon energy, Γ the band broadening factor, χ an arbitrary phase factor and $\Delta R/R$ the relative absorption modulation. The electro optic energy is given by:

$$(\hbar\theta)^3 = \frac{q^2\hbar^2F^2}{2\mu} \quad (2)$$

where F is the electric field and μ the reduced mass of electrons and holes. When EAM signals are dominated by heavy hole transitions, the internal field is extracted using Eq. (1) from the slope of $(4/3\pi)(E_n - E_g)^{3/2}$ versus n curves where E_n is the energy and n is the index of the extremum points in the EAM spectrum [3]. However, distinct interference beats, observed in Figs. 4 and 5, indicate that light hole transitions also contribute to the signal. We therefore used Fourier analysis [9] to distinguish between both transitions.

The Fourier transforms of the EAM signals measured at various bias levels are presented in Fig. 7. At high voltages, the heavy and light hole contributions can be clearly identified. However, at low bias levels, the curves are too broad to distinguish between both transitions.

In Eq. (1) we observe the multiplication of the cosine function by two additional terms. Each of these terms broadens the peaks in the Fourier domain (Fig. 7). We have therefore multiplied the measured EAM spectrum by $E^2(E-E_g)$ prior to the Fourier analysis. The result is demonstrated in Fig. 8, where significant reduction of the peak width is observed and the energy resolution is thus improved.

It is instructive to compare the ratio of electron–light hole and electron–heavy hole reduced masses obtained from our experiments to published data. The field dependence of the Fourier domain peak is [9]:

$$f_{\text{peak}} = \frac{2}{3\pi(\hbar\theta)^{3/2}} = \frac{2\sqrt{2\mu}}{3\pi q\hbar F} \quad (3)$$

and the ratio of the heavy hole and light hole peak positions is thus,

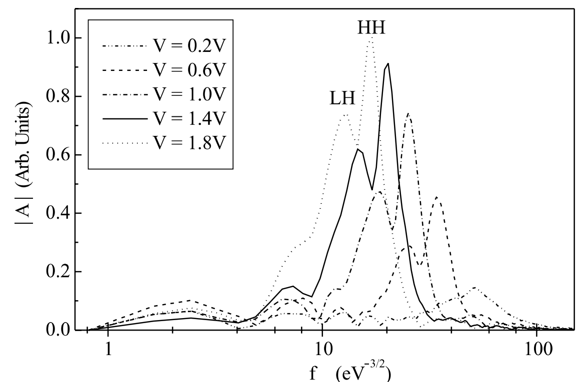

Fig. 7. Fourier transforms of EAM spectra measured at various bias levels. In each curve, the high-energy peak corresponds to heavy hole transition and the low energy peak to light hole transition.

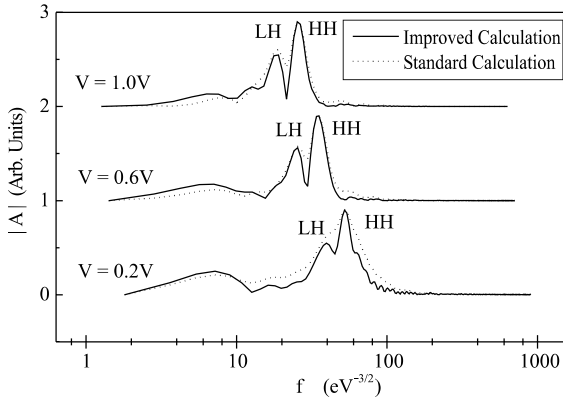

Fig. 8. Comparison of the Fourier transforms calculated with and without de-correlation. Enhanced resolution is obtained by the de-correlation method.

$$\frac{f_{\text{peak HH}}}{f_{\text{peak LH}}} = \sqrt{\frac{\mu_{\text{HH}}}{\mu_{\text{LH}}}} \tag{4}$$

The reduced mass ratio of 1.34 ± 0.04, calculated from the experimental data using Eq. (4), agrees well with published data [10].

The average electric field values calculated from the heavy hole peak locations using Eq. (3) are plotted in Fig. 9 versus the applied DC bias. The validity of our results can be verified by comparing the obtained electric field to the expected result [11]:

$$V_{\text{ext}} + V_{\text{bi}} = Fd + \frac{KT}{q} \tag{5}$$

where V_{bi} is the built in voltage and d the width of the depletion region. The thickness of the depletion region was obtained from the small signal capacitance of the reverse biased Schottky diodes. It was constant at all DC bias levels and equaled the nominal thickness of the undoped layer (140 nm). A plot of the measured electric field versus applied DC bias, must thus have a slope of 1/d. However, the slope of the curves in Fig. 9, is about 22% smaller than predicted by Eq. (5). In a similar experiment carried out in GaAs diodes, the obtained field magnitudes were 25% smaller than the predicted ones [12]. We therefore conclude that a refinement of the theory underlying the field extraction technique is required, and here simply use the slope of the curves given in Fig. 9 as a "calibration factor" of 0.78.

The built in voltages for the Pt and Ti Schottky diodes were obtained from the data in Fig. 9 by extrapolating the linear curves to zero field. Using this technique the linear field calibration and exact knowledge of the depletion layer width are not required. The results were $V_{\text{bi Pt}} \approx 0.54$ V and $V_{\text{bi Ti}} \approx 0.59$ V, indicating again a difference of about 50 meV in the Schottky barrier height at the metal semiconductor interface.

3.2. Current voltage characteristics of the Schottky diodes

The IV characteristics of the Pt and Ti Schottky diodes used in the EAM experiments are plotted in Fig. 10. Note that the turn on voltage of the Pt diode is lower than that of the Ti diode because of the smaller Schottky barrier height of the Pt contact. The barrier height can be extracted assuming thermionic emission (TE) using [13]:

$$\frac{I}{1-\exp(-qV/KT)} = A^{**}T^2 S \exp(-q(\phi_{\text{B}} - \Delta\phi_{\text{B}})/KT)\exp(qV/nKT) \tag{6}$$

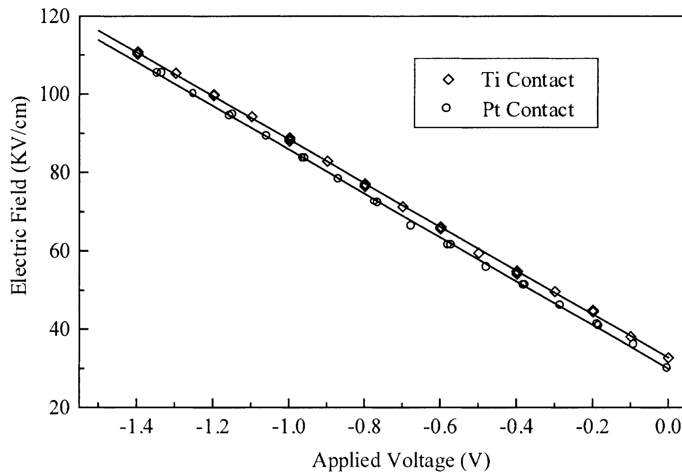

Fig. 9. Curves of the internal electric field versus the applied external voltage. Field magnitudes were calculated from the heavy hole peak locations in Fourier transforms of the de-correlated EAM spectra.

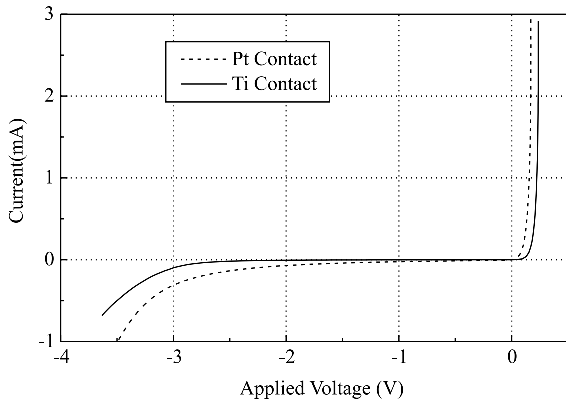

Fig. 10. Current–voltage characteristics of the Pt and Ti Schottky diodes.

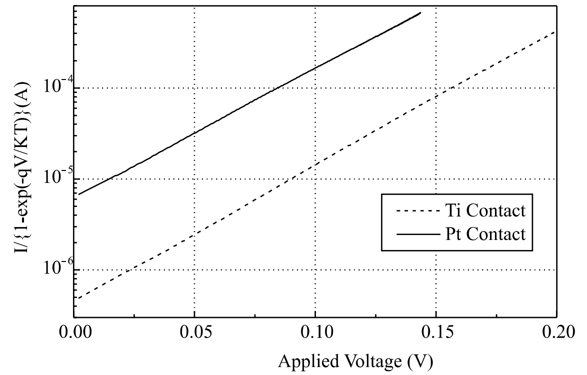

Fig. 11. Normalized Schottky diode forward current characteristics.

where A^{**} is Richardson's constant, ϕ_B is the Schottky energy barrier height, $\Delta\phi_B$ the image force lowering of the barrier, T the temperature, S the area of the device and n the ideality factor due to the barrier lowering effect.

In Fig. 11, $(I/1 - \exp(-qV/KT))$ is plotted as a function of applied voltage. Using a value of 61.9 AK^2/cm^2 for Richardson's constant [14] and taking into account the image force lowering at zero bias $\Delta\phi_{B0} \approx 10$ meV [13], the obtained Schottky barrier heights of Pt and Ti contacts were 0.48 and 0.55 eV respectively. These results are close to the results presented in Ref. [4].

In the IV experiments one measures the Schottky barrier heights. The energy difference between the valance band and the Fermi level in the heavily doped semiconductor ($\Delta E = E_f - E_V \approx 35$ meV [15]) must be added to the results to obtain the built-in voltage. The agreement with the built-in voltage values obtained from the EAM measurements is within the estimated experimental error (20 meV).

3.3. Specific contact resistance

The specific contact resistance of Pt to heavily doped GaInAs was measured using transmission line measurements (TLM) [16]. The thickness of the heavily doped layers was 50 nm. Since the contacts were not annealed, we assumed that the layer underneath the contacts was not modified by the deposition of the metals. The doping levels of the layers were measured by the Hall effect experiment. The obtained results are summarized in Table 1. The specific contact resistance of Ti based contacts was not measured since it is available in Ref. [17].

4. Discussion

Both the EAM and electrical measurements have revealed that the difference between the Schottky barrier height formed by the two metals is about 50–70 meV, a value much smaller than the work function difference of the two metals ($\Delta\phi_m \approx 1.3$ eV). Using Bardeen's model [18] this difference can be accounted for by a 10 Å thick interfacial oxide layer with 2×10^{14} cm^{-2} eV^{-1} surface states between the metal and semiconductor.

The small difference in the Schottky barrier height formed by the two metals agrees well with measurements performed by Kajiyama et al. [2] who detected Fermi level pinning at approximately two thirds of the energy gap in Au contacts to different compositions of $Ga_{1-x}In_xAs$ and disagrees with measurements performed by Brillson et al. [19] who found large differences between barrier heights of Au, Ge, Al and In contacts to $Ga_{0.47}In_{0.53}As$

Although the measured difference in the Schottky barrier heights of the two contacts is small, it explains a substantial difference in the specific contact resistance of these metals. Roughly, Pt contacts have a four times lower contact resistance than Ti contacts to p-type GaInAs. Since the effective mass of holes ($m^* = 0.43$) is relatively large, the characteristic energy E_{00} at room

Table 1
Specific contact resistance measured for Pt based contacts

	Be doping (cm^{-3})			Sn doping (cm^{-3})	
	10^{19}	2.7×10^{19}	5×10^{19}	10^{19}	8×10^{19}
ρ_c (Ωcm^2)	1.8×10^{-5}	8×10^{-7}	7×10^{-8}	4×10^{-7}	10^{-8}

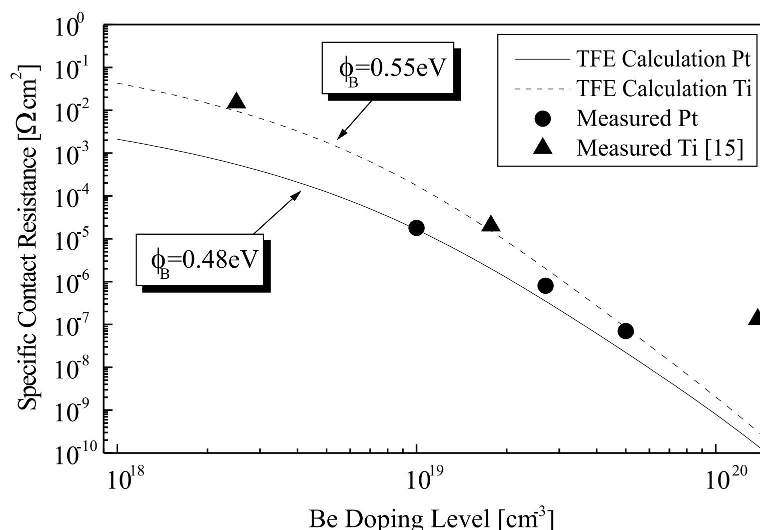

Fig. 12. Measured and calculated specific contact resistance. The metal–semiconductor energy barrier heights measured by the EAM technique were used in the calculation.

temperature is of the order of KT and thermionic field emission (TFE) transport dominates even for high doping levels. We have used the expression, derived by Yu [20], to calculate the specific contact resistance for Ti and Pt contacts. The measured Schottky barrier heights of 0.55 and 0.48 eV corrected by the image force lowering effect [13] were used in calculations. In Fig. 12, the calculated results are compared with the TLM results reported here for Pt based contacts and with results reported by Ressel et al. [17] for Ti based contacts. Good agreement between measurements and calculations is evident. However, for doping levels exceeding 3×10^{19} cm^{-3} the measured specific contact resistance values are higher than theoretically predicted. This result may be explained by the presence of oxide states that were not taken into account in the calculation.

Because of the small effective mass of electrons ($m^* = 0.041$) very low specific contact resistance values can be obtained to n-type GaInAs as presented in Table 1. The dominant transport mechanism in this case is field emission.

5. Conclusions

A thorough investigation of Ti and Pt based contacts to p-type GaInAs was performed using optical and electrical characterization techniques. EAM spectra were analyzed by an improved Fourier technique and the Schottky barrier height values were extracted. The results were compared to the Schottky barrier heights measured by IV characterization and good agreement was obtained.

The Schottky barrier height of the Ti contact was found to be 50–70 meV higher than that of the Pt contact. This result is significantly smaller than the work function difference (1.3 eV) but is consistent with the specific resistance ratio of Ti and Pt contacts to p-type GaInAs. The specific resistance of Pt contacts to p-type GaInAs is about four times lower than that of Ti contacts.

Acknowledgements

We thank D. Schoenman for packaging the samples and S. Cohen for technical support.

References

[1] Micheaelson HB. The work function of the elements and its periodicity. J Appl Phys 1977;48:4729–33.

[2] Kajiyama K, Mizushima Y, Sakata S. Schottky barrier height of $n - In_xGa_{1-x}As$ diodes. Appl Phys Lett 1973;23: 458–459.

[3] Pollak FH, Shen H. Modulation spectroscopy of semiconductors: bulk/thin films, microstructures, surfaces/interfaces and devices. Mater Sci Engng 1993;R10:275–374.

[4] Malacky L, Kordos P, Novak J. Schottky barrier contacts on $(p) - Ga_{0.47}In_{0.53}As$. Solid State Electr 1990;33:273–8.

[5] Hamm RA, Ritter D, Temkin H. Compact metalorganic molecular beam epitaxy growth system. J Vacuum Sci Technol 1994;A12:2790–4.

[6] Ren F, Abernathy CR, Pearton SJ, Lothian JR. Use of Ti in ohmic metal contacts to p-GaAs. J Vac Sci Technol B 1995;13:293–6.

[7] Aspnes DE, Studna AA. Schottky-Barrier electroreflectance: application to GaAs. Phys Rev B 1973;7:4605–25.
[8] Aspnes DE. Band nonparabolicities, broadening and internal field distributions: the spectroscopy of Franz–Keldysh oscillations. Phys Rev B 1974;10:4228–38.
[9] Wang DP, Chen CT. Fast Fourier Transform of Photoreflectance Spectroscopy of δ-doped GaAs. Appl Phys Lett 1995;67:2069–71.
[10] Adachi S. Material parameters in $In_{1-x}Ga_xAs_yP_{1-y}$ and related binaries. J Appl Phys 1982;53:8775–91.
[11] Sze SM. Physics of Semiconductor Devices. 2nd edition. New York:Wiley, 1981.
[12] Tober RL. Characterizing electric fields in (111)B and (100) p–i–n diodes. Phys Rev B 1997;55:16371–5.
[13] Rhoderick EH, Williams RH. Metal–semiconductor contacts. 2nd ed. Oxford: Clarendon Press; 1988.
[14] Veteran JL, Mullin DP, Elder DI. Schottky barrier measurements on p-type $In_{0.53}Ga_{0.47}As$. Thin Solid Films 1982;97:187–90.
[15] Aymerich-Humet X, Serra-Mesters F, Millan J. Adsh generalize approximation of the Fermi–Dirac integrals. J Appl Phys 1983;54:2850–1.
[16] Reeves GK, Harrison HB. Obtaining the specific contact resistance from transmission line model measurements. IEEE Electron Dev Lett 1982;EDL-3:111–3.
[17] Ressel P, Vogel K, Fritzsche D, Mause K. Nonalloyed ohmic contacts for P^+-type in GaAs base layer in HBTs. Electr Lett 1992;28:2237–8.
[18] Bardeen J. Surface states and recombination at a metal semiconductor contact. Phys Rev 1947;71:717–27.
[19] Brillson LJ, Slade ML, Viturro RE, Kelly MK, Tache N, Margaritondo G, Woodall JM, Kirchner PD, Pettit GD, Wright SL. Absence of Fermi level pinning at metal – $In_xGa_{1-x}As$ (100) interfaces. Appl. Phys. Lett. 1986;48: 1458–60.
[20] Yu AYC. Electron tunneling and contact resistance of metal–silicon contact barriers. Solid State Electron 1970; 13:239–47.